

The quark contents of the nucleon and their implication for dark matter search

C. Alexandrou^{ab}, M. Constantinou^b, V. Drach^{*cd}, K. Hadjiyiannakou^b, K. Jansen^c, G. Koutsou^a, A. Strelchenko^b and A. Vaquero^a

^a *Computation-based Science and Technology Research Center (CaStoRC), The Cyprus Institute, 20 Constantinou Kavafi Street Nicosia 2121, Cyprus*

^b *Department of Physics, University of Cyprus, P.O. Box 20537, 1678 Nicosia, Cyprus*

^c *NIC, DESY Zeuthen, Platanenallee 6, D-15738 Zeuthen, Germany*

^d *CP³-Origins & the Danish Institute for Advanced Study DIAS, University of Southern Denmark, Campusvej 55, DK-5230 Odense M, Denmark*
E-mail: drach@cp3.dias.sdu.dk

We present results concerning the light and strange quark contents of the nucleon using $N_f = 2 + 1 + 1$ flavours of maximally twisted mass fermions. The corresponding σ -terms are casting light on the origin of the nucleon mass and their values are important to interpret experimental data from direct dark matter searches. We discuss our strategy to estimate systematic uncertainties arising in our computations. Our preliminary results for the σ -terms read $\sigma_{\pi N} = 37(2.6)(24.7)\text{MeV}$ and $\sigma_s = 28(8)(10)\text{MeV}$. We present our recent final analysis of the y_N parameter and found $y_N = 0.135(46)$ including systematics[1].

*31st International Symposium on Lattice Field Theory - LATTICE 2013
July 29 - August 3, 2013
Mainz, Germany*

*Speaker.

1. Introduction

The various evidences for the existence of dark matter have led to the development of experiments dedicated to detect dark matter directly. The detection relies on the measurements of the recoil of atoms hit by a dark matter candidate. One popular class of dark matter models involve an interaction between a WIMP and a nucleon mediated by a Higgs exchange. Therefore, the scalar quark contents of the nucleon are fundamental ingredients in the WIMP-nucleon cross section. In this way, the uncertainties of the scalar quark contents translate directly into the accuracy of the constraints on beyond the standard model physics. Since the coupling of the Higgs to quarks is, through the Yukawa interaction, proportional to the quark masses, it is important to know how large the scalar quark matrix elements of the nucleon are, in particular for the strange and charm quarks.

One common way to write the parameters entering the relevant cross section are the so-called σ -terms of the nucleon:

$$\sigma_{\pi N} \equiv m \langle N | \bar{u}u + \bar{d}d | N \rangle \quad \text{and} \quad \sigma_s \equiv m_s \langle N | \bar{s}s | N \rangle, \quad (1.1)$$

where m denotes the light quark mass and m_s the strange quark mass. To quantify the scalar strangeness content of the nucleon a parameter y_N is introduced,

$$y_N \equiv \frac{2 \langle N | \bar{s}s | N \rangle}{\langle N | \bar{u}u + \bar{d}d | N \rangle}, \quad (1.2)$$

which can be also related to the σ terms of the nucleon in eq. (1.1).

The direct computation of the above matrix elements is known to be challenging on the lattice for several reasons. First, it involves the computation of "singlet" or "disconnected" diagrams that are very noisy. Second, discretisations that break chiral symmetry generally suffer from a mixing under renormalization between the light and strange sector, which is difficult to treat in a fully non-perturbative way.

However, as has been shown in [2], twisted mass fermions offer two advantages here: they provide both an efficient variance noise reduction for disconnected diagrams [3] and avoid the chirally violating contributions that are responsible for the mixing under renormalization in our setup. Note that a great effort has been spent developing techniques to estimate efficiently the relevant disconnected contribution (see for instance [4, 5, 6, 7, 8]).

In this work we present a preliminary analysis of the systematic errors occurring in the computation of the σ -terms defined in Eq. (1.1). More precisely we study the uncertainties associated to the excited states contamination, lattice cut-off effects and the chiral extrapolation. We also summarise our final results including all systematics for the y_N parameter as obtained in [1].

2. Results

2.1 Lattice techniques

In this study we use gauge configuration generated by the ETM collaboration. We use $N_f = 2 + 1 + 1$ ensembles with a number of light quark masses corresponding to pseudoscalar meson masses ranging from 220 MeV to 490 MeV and two lattice spacing, $a = 0.082$ fm and $a = 0.064$ fm, to examine lattice cut-off effects.

We refer to [9] for details on the gauge ensemble used in this work. In order to compute matrix elements involving strange quarks, we work within a mixed action setup introducing an additional doublet of mass degenerate twisted mass quarks of mass m_s in the valence sector.

The scalar quark matrix elements involved in Eq. (1.1) can then be computed using the asymptotic behaviour of a suitable ratio of three and two-point functions defined as

$$R_{O_q}(t_s, t_{\text{op}}) = \frac{C_{3\text{pts}}^{O_q}(t_s, t_{\text{op}})}{C_{2\text{pts}}(t_s)} = \langle N|O_q|N \rangle^{(\text{bare})} + \mathcal{O}(e^{-\delta m t_{\text{op}}}) + \mathcal{O}(e^{-\delta m(t_s - t_{\text{op}})}), \quad (2.1)$$

where O_q refers to the operator in which we are interested in, namely $O_l \equiv \bar{u}u + \bar{d}d$ and $O_s \equiv \bar{s}s$. In eq. (2.1), t_s refers to the source-sink separation and t_{op} to the source-operator separation. In addition, δm stands for the mass gap between the nucleon and its first excited state. From eq. (2.1) it is clear that large times t_{op} and t_s are needed to suppress the so-called excited state contributions. However, due to the exponential decrease of the signal-over-noise ratio at large times, it is numerically very expensive to obtain a good signal for increasing t_s or t_{op} .

The nucleon states themselves are created using smeared interpolating fields, which have already been optimized themselves to suppress excited state contaminations in the two point function.

For the precise expression of the operators O_q , their (solely) multiplicative renormalization properties and our computational techniques we refer the reader to [2]. In the following we discuss our analysis strategy to obtain results extrapolated to the physical pion mass and to estimate the systematic errors.

2.2 σ -terms

As discussed in [10], contributions from the excited states in Eq. (2.1) are not negligible both in R_{O_l} and R_{O_s} . We illustrate this in Fig. 1 and 2, where we show the dependence of the ratio Eq. (2.1) when t_s is increased for R_{O_l} (left) and R_{O_s} (right). In the light sector we observe a shift of $\sim 22\%$ in the value of $R_{O_l}(t_s, t_s/2)$ when increasing t_s from 0.98 fm to 1.48 fm. In the strange sector, increasing t_s from 0.98 fm to 1.6 fm, changes $R_{O_s}(t_s, t_s/2)$ by about $\sim 80\%$. Therefore, with the improved statistics employed here, it is not clear that the (time) asymptotic regime of Eq. (2.1) is reached. In order to nevertheless estimate the asymptotic values of the matrix elements, we performed extrapolations of the lattice data to infinite source-sink separations. This step requires extrapolation that leads to an additional systematic error previously neglected in other computations.

We first describe our strategy to extrapolate the lattice data of R_{O_s} to $t_s \rightarrow \infty$ to infinite source-sink separation. Since we have data for every source-sink separation t_s , we choose to perform fits to the following function :

$$f(t_s, t_{\text{op}}) \equiv A(t_{\text{op}}) + B(t_{\text{op}})e^{-\delta m t_s} \quad (2.2)$$

where A and B depend on the operator source-operator separation t_{op} of Eq. (2.1). Note that we assume that only one excited state contributes in our fitting range. For large enough t_{op} , A will become time independent and the corresponding constant value provides the desired bare matrix element. In order to have stable fits we fix t_{op} and perform fits for a range of $t_s \in [t_s^{\text{min}}, t_s^{\text{max}}]$ and for a fixed value of δm . Each choice of $\{t_{\text{op}}, [t_s^{\text{min}}, t_s^{\text{max}}], \delta m\}$ will lead to a result for the extrapolated data. In order to estimate the systematic error due to the excited states contamination we thus vary

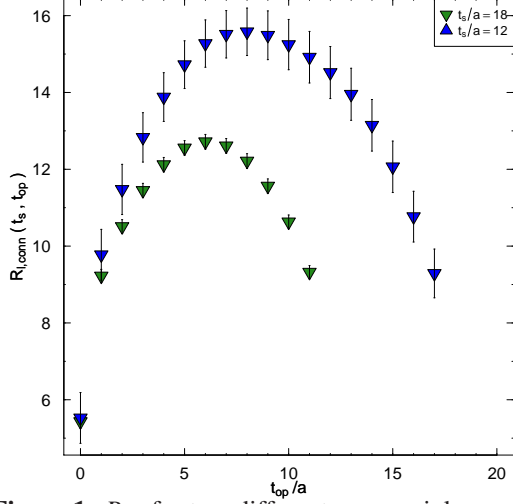


Figure 1: $R_{l,conn}$ for two different source-sink separations $t_s = 12a \sim 0.98$ fm and $t_s = 18a \sim 1.48$ fm on a $32^3 \times 64$ lattice with a pseudoscalar mass of ~ 355 MeV

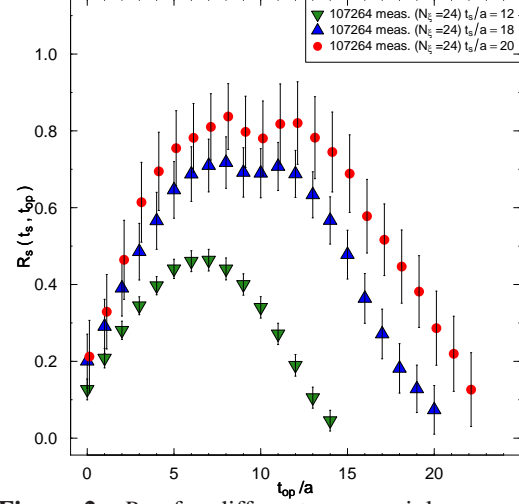


Figure 2: R_{O_s} for different source-sink separations ranging from $t_s \sim 0.98$ fm to $t_s \sim 1.6$ fm on a $32^3 \times 64$ lattice with a pseudoscalar mass of ~ 392 MeV

Type I	$t_{op}^1 \sim 0.66$ fm	$\sim [0.98, 1.48]$ fm	$\delta m^1 \approx 360$ MeV
Type II	$t_{op}^2 \sim 0.94$ fm	$\sim [1.15, 1.48]$ fm	$\delta m^1 \approx 360$ MeV
Type III	$t_{op}^1 \sim 0.66$ fm	$\sim [0.98, 1.48]$ fm	$\delta m^2 \approx 600$ MeV
Type IV	$t_{op}^2 \sim 0.94$ fm	$\sim [1.15, 1.48]$ fm	$\delta m^2 \approx 600$ MeV

Table 1: Parameters used for the extrapolation to infinite source-sink separation. Two values of δm are considered, one is fixed according to the experimental mass splitting between N and N^* , and the other is estimated from fits of the two-points function. In practice the values of t_{op} , t_s^{min} and t_s^{max} are slightly varied on each ensemble in order to have stable fits.

all of them. For the preliminary analysis presented here, four types of extrapolations denoted by I, II, III and IV, depending on the choice of the parameters as summarized in Table 1

An example of such an extrapolation for $t_{op} = 0.82$ fm and $t_{op} = 1.23$ fm is shown in Fig. 3. The values of $A(t_{op})$ are shown by horizontal black lines. We have repeated this procedure on every ensemble resulting in the corresponding values of σ_s for all four types of extrapolation considered, as can be seen Table 1. Note that the values of t_{op} used in the table are smaller than the one considered in Fig. 3 in order to have stable fits on all ensembles. For the type I extrapolation we show in Fig. 4 the chiral behaviour of σ_s for all our ensembles employing two different lattice spacings. As can be seen comparing the green ($a = 0.064$ fm) and blue triangles ($a = 0.082$ fm), lattice cut-off effects are not visible at the present level of accuracy. The extrapolations to the physical pion mass are carried through using two linear fits in m_{PS}^2 excluding or not data obtained for $m_{PS} > 400$ MeV. The spread of the results at the physical pion mass, using type I, II, III, IV allow us to estimate the systematic error coming from excited states contamination. The difference between the two chirally extrapolated values provides an estimate of the systematic uncertainty associated with the chiral extrapolation. Our preliminary result reads $\sigma_s = 28(8)(10)$ MeV where the first error is statistical and the second is the systematic error stemming from both excited states and chiral extrapolation. This value is fully compatible with the bound on σ_s computed in ref. [1].

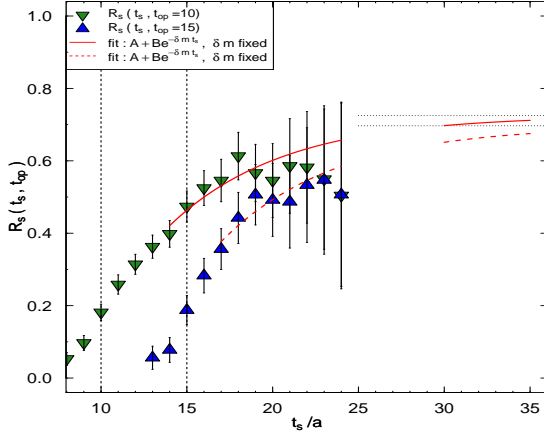


Figure 3: Extrapolation of $R_{O_s}(t_s, t_{op})$ to large times t_s for two values of t_{op} and for δm fixed to the experimental mass splitting between the nucleon N and the first excited state N^* . The gauge ensemble is the same as the one used in Fig. 1

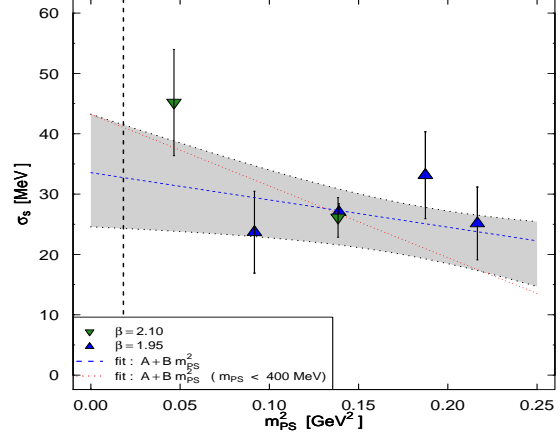


Figure 4: Chiral behaviour of σ_s as a function of m_{PS}^2 . Data at two lattice spacings are shown as well as a linear extrapolation (dotted blue line) and its corresponding error band. The physical point is denoted by a vertical dashed line.

In the case of the light σ -term, $\sigma_{\pi N}$, we have performed the extrapolation in t_s of type I to IV only for the disconnected part. For the connected part, which is the dominant contribution, we do not have access to the full source-sink time dependence of R_{O_l} . Instead, we consider two ways to estimate the systematic error due to the excited states contamination in the connected part. In the case denoted *C* we use the results obtained with $t_s = 0.98$ fm and can not resolve the contribution of the excited states in the connected part. In the case *D*, we used the only ensemble for which data at several source-sink separation are available ($a = 0.082$ fm and $m_{PS} \approx 355$ MeV) to estimate the excited states contamination in the connected part by comparing results obtained at $t_s = 0.98$ fm and $t_s = 1.47$ fm. We deduce that the size of the excited states contribution is 18%. Assuming that this effect does not depend on the value of the pseudoscalar mass, we shift the lattice data on all the other ensembles by 18%. We then perform chiral extrapolations using the results of cases *C* and *D*. Combining these results with the combinations methods I to IV for the disconnected part allows us to at least estimate the systematic error due to the excited states contamination.

In the case of $\sigma_{\pi N}$ the dependence as a function of m_{PS}^2 is not negligible. In Fig. 5 we show our results for $\sigma_{\pi N}$ as a function of m_{PS}^2 and for two lattice spacings using type I extrapolations for the disconnected parts and a fixed source-sink separation of $t_s = 0.98$ fm for the connected part (previously referred as case *C*). We furthermore indicate the physical point by a vertical dashed line. Using the well known baryon chiral perturbation theory result $m_N = m_N^0 + c_0 m_{PS}^2 + c_1 m_{PS}^3$ with $c_1 = -\frac{3g_A^2}{16\pi f_\pi^2}$ and using the relation (true in chiral limit) $\sigma_{\pi N} = m_{PS}^2 \frac{\partial m_N}{\partial m_{PS}^2}$, we show by a blue dotted line a fit of the data given by

$$\sigma_l = m_{PS}^2 \left(c_0 + \frac{3}{2} c_1 m_{PS} \right) \quad (2.3)$$

where the coefficient c_0 is the only fitting parameter and c_1 is fixed and deduced from the chiral expansion in HB χ PT of the nucleon mass. Inspecting Fig. 5, when performing such a fit, even restricting ourselves to $m_{PS} < 400$ MeV, the fit does not describe the data. In order to obtain a

description of the data, we add a term m_{PS}^4 to Eq. (2.3) with a free coefficient that is to be fitted. This fit describes the data indeed satisfactory as shown in Fig. 5. Also, in this case including or not data with pseudoscalar meson masses larger than 400 MeV gives consistent results (see the red dashed line and the full black line in Fig. 5). We estimate the systematic error coming from the chiral extrapolation by comparing the extrapolation of a linear (obtained from Eq. (2.3) setting $c_1 = 0$) and quartic fit. We find $\sigma_{\pi N} = 37(2.6)(24.7)$ MeV where the first error is statistical and the second is our estimate of the systematic errors due to the chiral extrapolation and to the excited states contamination.

2.3 y_N parameter

We summarize here briefly our analysis of the y_N parameter. Contrary to the σ -terms, y_N can be obtained directly by a ratio of three point function. We show in Fig. 6 our results for y_N as a function of m_{PS}^2 . Data for several source-sink separation are shown as well as for two lattice spacings. We observe that data obtained at different source-sink separations (filled and empty triangle) indicate that the excited states contamination is non negligible and about 32%. The excited states contamination is thus small compare to the excited states contamination in the determination of σ_s which must partly cancel in the ratio used to compute y_N . We also show the result obtained for a different lattice spacing in the same range of pseudoscalar mass (empty circle) to indicate that lattice cut-off effects are not a dominant source of systematic errors. We then perform a leading order (linear in m_{PS}^2) and an extrapolation adding a m_{PS}^4 term to the fit formula to estimate the error introduced by the chiral extrapolation. Note that the empty symbols are not included in the fits and are only shown to estimate systematic errors. Our final result is (including systematic errors) $y_N = 0.135(46)$. We refer to [1] for more details on this analysis.

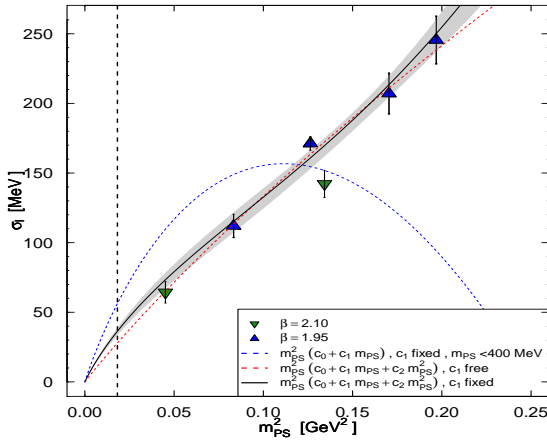


Figure 5: Chiral behaviour of σ_s as a function of m_{PS}^2 after extrapolation of type I-C. We show data at two lattice spacings. As explained in the text we show cubic and quartic fits. The physical point is denoted by a vertical dotted line.

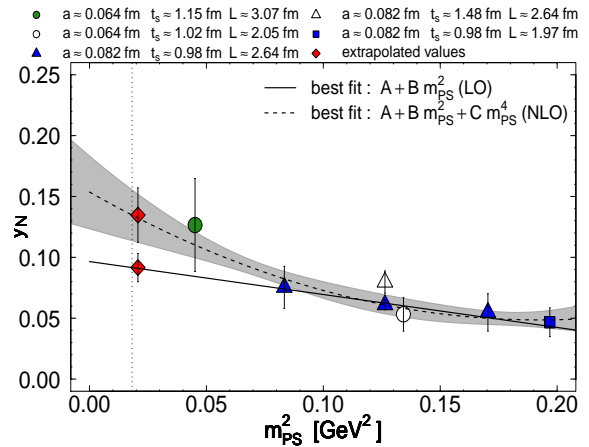


Figure 6: Our results for y_N as a function of m_{PS}^2 for two values of the lattice spacing for several fixed source-sink separation t_s as given in the legend. We extrapolate to the physical value of the pion mass using linear and quadratic fits in m_{PS}^2 . For the quadratic fit, we also show the corresponding error band.

3. Conclusion

In this proceedings contribution we have presented our results concerning the nucleon light and strange σ -terms. We discussed in detail the analysis of the systematic effects in a direct computation of these matrix elements. In particular, we showed that a large excited states contamination is present in the determination of the scalar quark matrix elements of the nucleon. This is the first time that a careful assessment of excited states contributions to the σ -terms has been carried out resulting into a systematic which is larger than the statistical error and must thus be considered in the evaluation of these quantities. We have also shown that lattice cut-off effects do not affect our results at the present level of accuracy. Another source of systematic effects in the case of $\sigma_{\pi N}$, which we have taken into account, is the chiral extrapolation. Our results for the σ -terms read $\sigma_{\pi N} = 37(2.6)(24.7)$ MeV and $\sigma_s = 28(8)(10)$ MeV. We summarised our recent analysis of the y_N parameter and found $y_N = 0.135(46)$ including systematic errors. This estimate provides a reliable input for dark matter models and experimental searches.

Acknowledgments

This work was performed using HPC resources provided by the JSC Forschungszentrum Jülich on the Juqueen supercomputer. It is supported in part by the DFG Sonderforschungsbereich/ Transregio SFB/TR9. Computational resources were partially provided by the Cy-Tera Project NEA ΥΠΟΔΟΜΗ/ΣΤΡΑΤΗ/0308/31 funded by the Cyprus Research Promotion Foundation (RPF). A. V is supported by the Cyprus RPF under the grant ΠΡΟΣΕΛΚΥΣΗ/ΝΕΟΣ/0609/16.

References

- [1] C. Alexandrou, M. Constantinou, S. Dinter, V. Drach, K. Hadjiyiannakou, K. Jansen, G. Koutsou and A. Vaquero, arXiv:1309.7768 [hep-lat].
- [2] S. Dinter, V. Drach, R. Frezzotti, G. Herdoiza, K. Jansen and G. Rossi, JHEP **1208**, 037 (2012) [arXiv:1202.1480 [hep-lat]].
- [3] K. Jansen *et al.* [ETM Collaboration], Eur. Phys. J. C **58**, 261 (2008) [arXiv:0804.3871 [hep-lat]].
- [4] C. Alexandrou, V. Drach, K. Hadjiyiannakou, K. Jansen, G. Koutsou, A. Strelchenko and A. Vaquero, arXiv:1211.0126 [hep-lat].
- [5] M. Engelhardt, arXiv:1210.0025 [hep-lat].
- [6] H. Ohki, *et al.* [JLQCD Collaboration], arXiv:1208.4185 [hep-lat].
- [7] G. S. Bali, P. C. Bruns, S. Collins, M. Deka, B. Glasle, M. Gockeler, L. Greil and T. R. Hemmert *et al.*, * Nucl. Phys. B **866**, 1 (2013) [arXiv:1206.7034 [hep-lat]].
- [8] C. Alexandrou, M. Constantinou, V. Drach, K. Hadjiyiannakou, K. Jansen, G. Koutsou, A. Strelchenko and A. Vaquero, arXiv:1309.2256 [hep-lat].
- [9] R. Baron, P. Boucaud, J. Carbonell, A. Deuzeman, V. Drach, F. Farchioni, V. Gimenez, G. Herdoiza *et al.*, JHEP **1006**, 111 (2010). [arXiv:1004.5284 [hep-lat]].
- [10] C. Alexandrou, M. Constantinou, S. Dinter, V. Drach, K. Hadjiyiannakou, K. Jansen, G. Koutsou and A. Strelchenko *et al.*, PoS LATTICE **2012**, 163 (2012) [arXiv:1211.4447 [hep-lat]].